SURFACE TEMPERATURE MAP OF JUPITER BEACH, EAST FLORIDA, USA USING LANDSAT 8 THERMAL INFRARED IMAGE

REMOTE SENSING OF ENVIRONMENT

GRADUATE CLASS PROJECT

FALL 2019

SUBMITTED BY

JYOTHIRMAYI PALAPARTHI

ABSTRACT

Coastal regions been one of those important locations now-a-days for the livelihood of many people for the scenic beauty and also the serenity and pleasant stay. This made increase in population to the beautiful coastal cities which increasing the temperature at these cities. However regular monitoring of temperature helps to notice the major reasons of it and also to take control measures to prevent the contribution of urban coastal cities to the global warming. Land surface temperatures are also important for land surface and atmosphere exchange. Also, the increase in temperature effect the environment as well as many habitants close to the coast and also within the urban cites. Temperature monitoring with the regular in-situ field measures for the vast area is a huge task. Remote sensing been playing a great role in monitoring the temperature of large areas. Study of Landsat images and their analysis in ArcGIS has become a big part in the temperature monitoring and made easy with less hassle of field work. The objective of the project is to study the surface temperature of the Jupiter beach (September 4th 2016) from a Landsat 8 Thermal Infrared Sensor 1 (TIRS 1) Collection Level. Also, the study includes the close look at the beach temperatures which are important to study as the temperature play a big role in sea turtle nesting success rate and also the sex determination. Finally, the study also includes the comparison of in-situ beach temperature measurements and analyzed Landsat data and to see the compatibility such that future measurements can be considered with or without the field measurements.

INTRODUCTION AND LITERATURE REVIEW

As atmosphere and earth climate is increasingly effected by the increase in temperature it is very important to monitor the land surface temperature which plays an important role in land surface energy budget and to understand land surface sensible heat and heat fluxes (Crago and Qualis, 2014). Land Surface Temperature is also an important aspect in many other study areas

like hydrological and agriculture land use, global climate change, and urban use of land use (Avdan and Jovanovska, 2016). The temperature variation also plays an important role in understanding the urban heat island effect which is described as built up areas that are hotter than nearby rural areas which are within a few miles apart by USEPA (United States Environmental Protection Agency). Consolidated surfaces and highly constructed areas in urban areas change the local climate and temperatures through the urban heat island effect (Oke 1987; Quattrochi and Ridd 1994), thus impacting the regional-scale consequences (Kalnay and Cai 2003).

Many major cities are hotter than their surroundings for many reasons, including the greater radiation from surfaces, the greater emission of heat, the thermal mass of buildings, the reduced evapotranspiration from soil, and the unusual pattern of convection (Roth, 2002). Another major reasons for the Urban heat islands—increased temperatures just within the urban areas is proportional logarithmically to the increase in the population of a city (Oke, 1973). In the world's largest cities, the difference between urban and rural temperatures is as much as 12°C. Urban warming likely has widespread biological consequences; because the environmental temperatures have been linked to temporal patterns of growth, survival and reproduction (Huey et al., 1979, Angilletta et al., 2002, Savage et al., 2004) to spatial patterns of body size, population density, and species diversity (Angilletta et al., 2004, Brown et al., 2004, Wiens et al., 2006). Urban heat islands should not only concern ecologists who wish to manage urban populations, but they should also interest physiologists who seek to test theories of thermal adaptation.

Populations of turtles in more southern parts of the United States are currently highly female biased and are likely to become ultra-biased with as little as 1°C of warming and experience extreme levels of mortality if warming exceeds 3°C. A change of 1–2°C can make a considerable difference to the sex ratio of the hatchlings and also the incubation success rate (Mrosovsky et al.,

1980) With all the importance to identify the surface temperatures it is important to obtain the surface temperature data and analyze to understand the reasons and what factors influence the more temperature changes in urban cities to take necessary measures for future climatic changes.

Field surface temperatures include the calculation of temperatures form the wind velocity (Aya et al., 2003), evapotranspiration and many other energy balance equations. The in situ temperature measures were also made through the double wire probe (Honami et al., 1992), HOBO temperature deploys and many other instruments. All the instruments used requires intense field labor and monitoring of the deployed instruments frequently to update the requirements and to obtain the data. However, the field temperature measurements can obtain the temperatures at different depths by installing the temperature logs at different depths.

There been an increase in awareness among the environment scientists that the remote sensing been playing an important role in obtaining data that is need to assess the environment in large scales and specific scales (Ustin, 2004). The calculation of surface temperature from remotely sensed images is much needed because it is an important factor controlling most physical, chemical, and biological processes of the Earth (Becker et al., 1990). These physical properties are difficult to monitor solely with in-situ instruments. Satellite borne instruments provide quantitative physical data at high spatial and temporal resolutions. Visible and near infrared remote sensing have been used extensively differentiate between city growth, landuse and landcover changes, vegetation index and population statistics. However, the satellite imaging for the climate changes and temperature variation been used in limitation with the thermal infrared and microwave radiations with urban surfaces and atmospheres. The use of satellite infrared remote sensing in estimating the surface physical properties and variables has been investigated by Carlson et al. (1981), Balling and Brazel (1988), Dousset, 1991, Roth et al. (1989), Quattrochi and Ridd

(1994), Owen et al. (1998), and Voogt and Oke (1998). Multi-sensor datasets, higher resolution and new processing techniques, have recently improved the accuracy of satellite thermal sensing, allowing new applications to urban climatology. Recent use of higher resolution a new processing techniques have recently improved the accuracy of the thermal image sensing and its new applications for the urban climatology.

OBJECTIVES OF THE STUDY

The main objective of the project is to analyze the surface temperature variation in Jupiter, FL using the Landsat 8 thermal image. Second objective is to have closure look at the temperatures at Jupiter North (South of the Jupiter inlet) and compare the results to the in-situ temperature data of the same day. Third objective is to measure the reflectance of the sediment sample at study location and comparing the reflectance curves to the temperature data.

DATA AND METHODOLOGY

Data:

The data was obtained from the USGS Earth Explorer. The data used was the Landsat 8 Thermal Infrared Sensor (TIRS) image. Thermal Infrared Sensor (TIRS) image. Landsat 8 program is jointly managed by the NASA and USGS which provides the satellite data and is publically available. This satellite collects about 400 new scenes comprising of400GB of data every day and the processed data is available for public. The Landsat 8 satellite orbits the the Earth in a sun-synchronous, near-polar orbit, at an altitude of 705 km (438 mi), inclined at 98.2 degrees, and circles the Earth every 99 minutes. The satellite has a 16-day repeat cycle with an equatorial crossing time: 10:00 a.m. +/- 15 minutes. Landsat 8 is instrumented with Operational Land Imager (OLI) which was built by Ball Aerospace and Technologies Corporation provides the data in nine

spectral bands ranging from Band 1 to Band 9 also including pan band. OLI captures data with improved radiometic precision over a 12-bit dynamic range, which improves overall signal to noise ratio. This translates into 4096 potential grey levels, compared with only 256 grey levels in Landsat 1-7 8-bit instruments. Improved signal to noise performance enables improved characterization of land cover state and condition. +The second instrument incorporated with Landsat 8 is Thermal Infrared Sensor (TIRS). TIRS was built by NASA Goddard Space Flight center. The TIRS have two spectral bands Band 10 (TIRS 1) and Band 11 (TIRS 2). The data used for the project to obtain the surface temperature is TIRS level 1 which is spectral Band of 10.

Methodology:

Remote sensing temperature measurements:

The Landsat 8 level 1 data is converted to temperature using the conversion to Top of Atmosphere (TOA) Radiance using the coefficients provided in the metadata file delivered with the level 1 product. The thermal constants which are available in the metadata are used to convert the thermal band data to TOA brightness temperature. Landsat Collections Level-1 data products consists of quantized and calibrated scaled Digital Numbers (DN) representing the multispectral image data. Landsat 8 products data acquired by both the Operational Land Imager (OLI) and Thermal Infrared Sensor (TIRS) are delivered in 16-bit unsigned integer format. Landsat 1-7 products are generated from single sensor data and are delivered in 8-bit unsigned integer format. Specific to Landsat 8, since the satellite's launch in 2013, energy from outside the normal field of view (stray light) has affected the thermal data collected by both thermal bands. The amount of stray light varies throughout each scene, depending upon radiance outside the instrument field of view. The stray light correction applied to Landsat 8 Collection 1 Level-1 data substantially improves image

uniformity and absolute calibration in typical scenes (USGS Landsat 8 Level 1 info). The conversion to TOA Radiance is obtained from the following equations.

Landsat Level-1 data can be converted to TOA spectral radiance using the radiance rescaling factors in the MTL file:

$$\mathbf{L_\lambda = M_L Q_{cal} + A_L}$$

where:

$\mathbf{L_\lambda}$ = TOA spectral radiance (Watts/(m^2 * srad * μm))

$\mathbf{M_L}$ =Band-specific multiplicative rescaling factor from the metadata (Radiance_Mult_Band_x, where x is the band number in this case x is 10).

$\mathbf{A_L}$=Band-specific additive rescaling factor from the metadata (Radiance_Add_Band_x, where x is the band number, in this case x is 10).

$\boldsymbol{Q_{cal}}$ = Quantized and calibrated standard product pixel values (Digital Number (DN)

Radiance Multiplier and Radiance add for the band 10 are 0.000334 and 0.1 respectively obtained from the metadata (Table 1). So the formula used to calculate the radiance (L_λ) is

$$\mathbf{0.0003342 * Q_{cal} + 0.1} \qquad \text{(Equation 1)}$$

The radiance is converted to the TOA Brightness temperature using the formula mentioned below.

$$\mathbf{T = K_2 / \ln(K_1 / L_\lambda + 1)} \qquad \text{(Equation 2)}$$

where:

T = Top of atmosphere brightness temperature (K)

L_λ =TOA spectral radiance (Watts/(m2 * srad * μm)

K_1 =Band-specific thermal conversion constant from the metadata (K_1_Constant_Band_x, where x is the thermal band number , in this case x is 10)

K_2 =Band-specific thermal conversion constant from the metadata (K_2_Constant_Band_x, where x is the thermal band number, in this case x is 10)

The values of K1 and K2 are obtained from eh metadata as shown in Table 1.

Table 1: Constants used in conversation to radiance and temperature.

	BAND 10	BAND 11
Radiance Multiplier	0.0003342	0.0003342
Radiance Add	0.1	0.1
K_1	774.89	480.89
K_2	1321.08	1201.4

As, the image used in the project is Band 10 the constants used are taken from the appropriate columns and combined the equation 1 and equation 2.

$$\mathbf{T= K_2/\ln (K_1/ (0.0003342*Q_{cal} +0.1) + 1)} \quad \text{(Equation 3)}$$

After using the constants of Band 10 the following formula is obtained to calculate the temperature in Kelvin.

$$\mathbf{T=1321.08/\ln (774.89/(0.0003342*Q_{cal}+0.1) +1)} \quad \text{(Equation 4)}$$

The data used was the Landsat 8 Level 1 (Band 10) which was collected on September 4th 2016 to obtain the surface temperatures and for the further analysis.

The study area chosen the project consists of whole stretch of Palm Beach county focusing on the Jupiter beach for the beach surface temperature analysis. The Landsat image was added to the ARC GIS 10.6.1. the raster image is used to derive the temperature using the raster calculator. The raster calculator is used to the conversion using the equation 4 to obtain the temperature estimation for the chosen location. The output raster is added to the Arp map and the color scheme ranging from blue for low temperatures to red for high temperatures is chosen form the Symbology.

In-situ field temperature data

The data used for the in-situ filed temperature was obtained from DR. Briggs lab. The data was collected form the HOBO temperature logs. The logs were deployed for every 15 days and placed back in at depths of 45 cm and 70 cm which replicate the actual sea turtle incubation chambers. The temperature data is collected every five minutes and the data is transferred to the computers every fifteen days for the further analysis. However, the surface temperature cannot be calculated using the HOBO data logs.

Reflectance measurements

As the temperature is inversely related to reflectance (Vincent et. al., 1997) reflectance for the one of the surface samples is obtained from the AMD spectrometer. Though the reflectance is also depended on the grain size, carbonate content for this particular project it is only compared to the temperature. The reflectance data is obtained for my dissertation work which seems appropriate for the project so it is been used in here. The reflectance measurements were obtained from ASD Sprectroradiometer Field Spec 3. Spectral reflectance between 350-2500 nm at 1 nm resolution was used to get the data. Five signatures were collected for each sample and then a splice correction was performed for a noted instrument sensitivity drift at the short wave near infrared. Then the

ASD binary files to ASCII format. These steps were done in the ASD Viewspec Pro software. Next, the five signatures were averaged each sample in Excel in order to remove electronic noise or any possible variations in lighting.

RESULTS

The Landsat 8 TIRS 1 map and the surface temperature map shown obtained using the equation 4 in raster calculator to obtain the temperature values is shown in Figure 1. Figure 1, top image shows the TIRS 1 map downloaded from the USGS Earth Explorer. The image below in Figure shows the surface temperature map of the study area showing red color in the high density areas and showing the medium temperatures (yellow color) at low density populated locations. Whereas water and lakes shown blue indicating the cooler temperature.

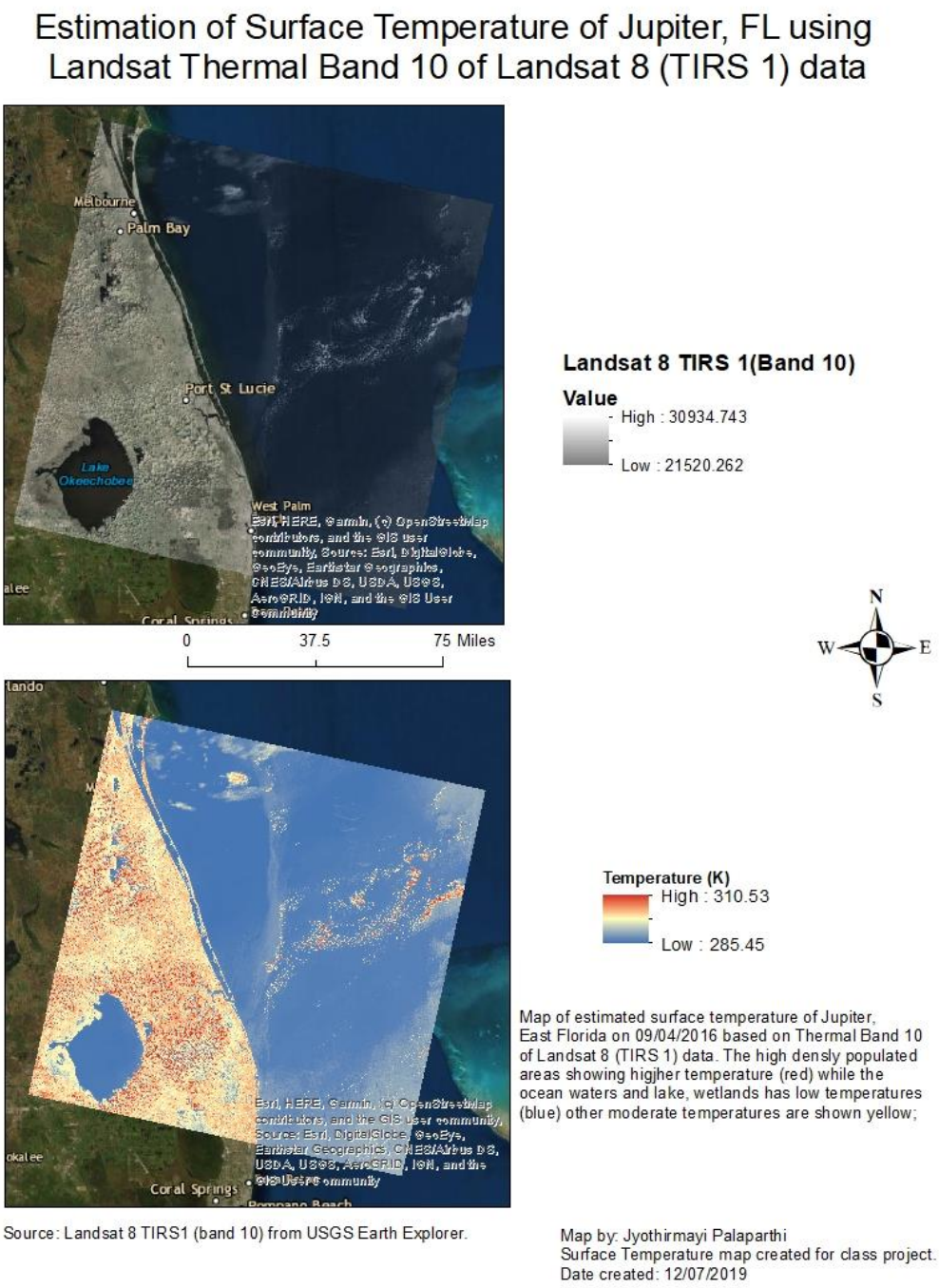

Figure 1: Landsat 8 (TIRS 1) Band 10 image on top and Surface temperature map of the study area on bottom.

The close zooming into the Jupiter North location of the map with classified Symbology is shown in Figure 2. The temperature values of the Jupiter location are seen to be ranging from 82.07°F to 90.88°F.

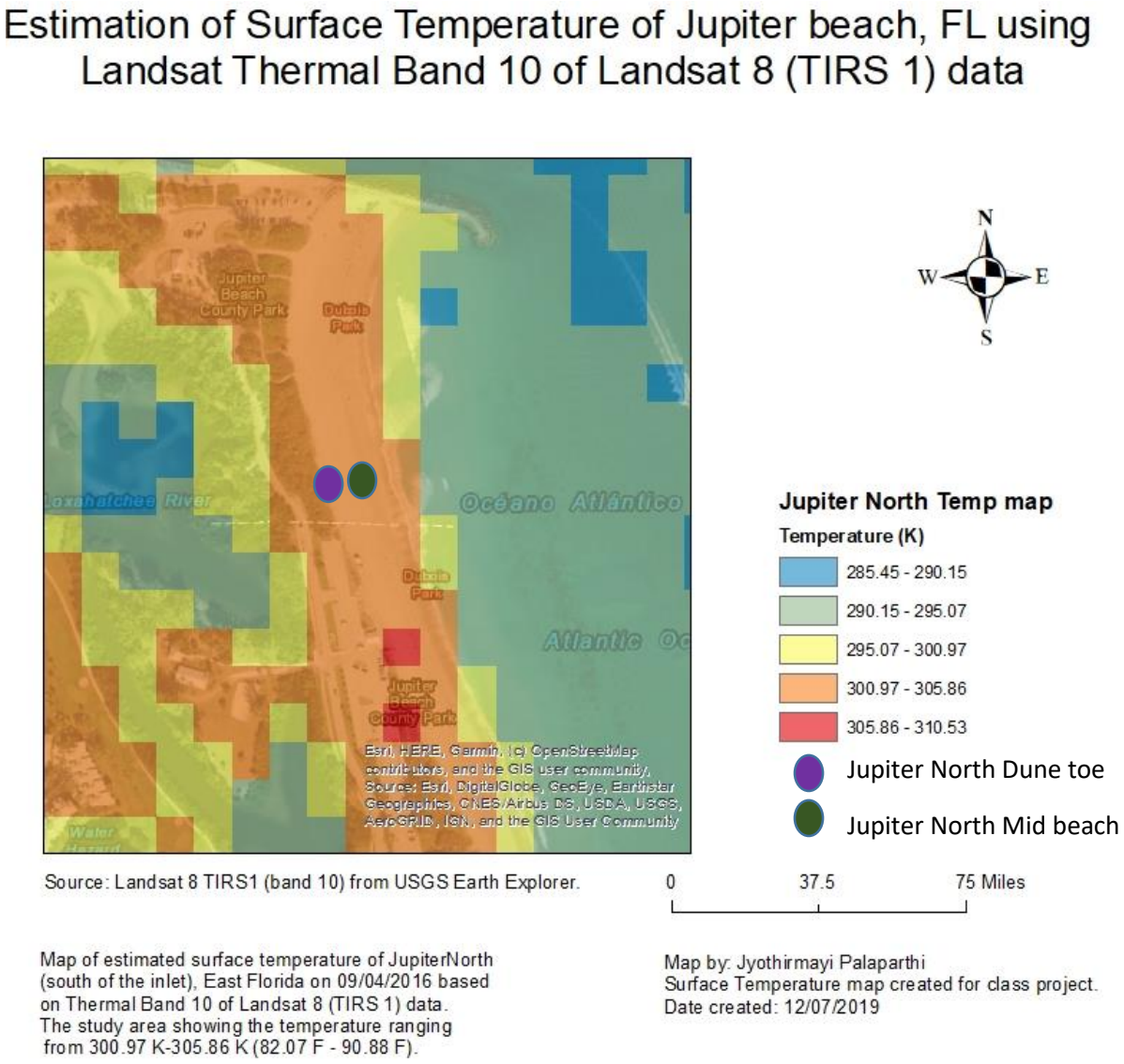

Figure 2: Jupiter North Beach surface temperatures.

The in-situ field measurements obtained using the HOBO temperature data logger for September 4th 2016 at 45 cm depth are shown in Appendix 1. The average temperature of the day for M45 (Mid beach at 45cm depth) and H45 (Dune toe at 45 cm depth) are shown in Table 2.

Table 2: Average temperature of whole day (09/04/2016) of Jupiter North at M45(mid beach at 45 cm) and H45 (Dune toe at 45cm).

Date	Avg Temp (°F)_M45	Avg Temp(°F)_H45
09/04/2016	88.506	87.772

The reflectance graph for the surface sediment sample of Jupiter at Dune toe and mid beach are obtained from the laboratory using AMD spectrometer is shown in Figure 3. The sediment samples used for the reflectance measurements were collected on 16th September 2016.

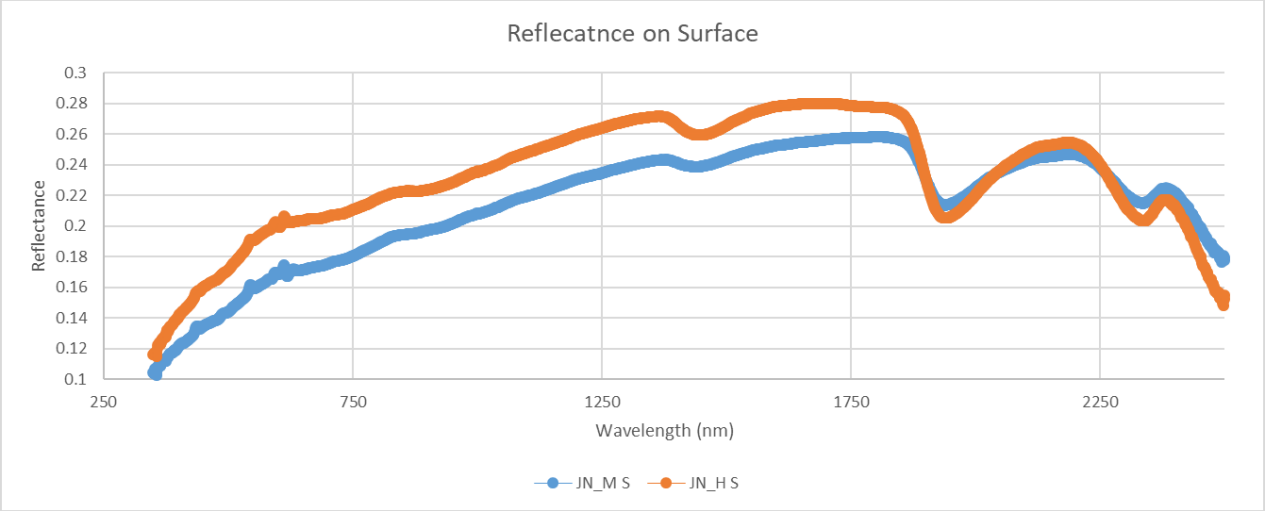

Figure 3: Reflectance graphs for the surface samples of Jupiter North at Mid beach and Dune toe.

DISCUSSIOJN

The temperature map of Jupiter north location in Figure 2 shows that the temperature is varying from 80.33 °F to 89.33 °F. The temperature values obtained from the field in-situ measurements show 88.51 °F and 87.77 °F (Table 2) respectively for Mid beach and Dune toe at 45cm depth. The values shown form the surface temperatures obtained through the remote sensing data and the filed measurements vary slightly because of the data collected in different dates and

also the surface temperatures and compared to the temperatures at depth of 45 cm. The reflectance graphs shown in Figure 3 show high reflectance for the H45 surface sediments that the sediments form M45. The temperature values show inverse correlation with the reflectance. Hence the low reflectance justifies the high temperatures.

CONCLUSIONS

The surface temperature maps are very important to differentiate the population density, vegetation, land use and land cover data. The analysis helps to monitor the temperature variation spatially and thus draw conclusions for the reasons of the increase in temperature regionally and also in global scale by looking at the regional contribution to it. The coastal use of the surface temperature maps helps to see the surface temperature of the beach and thus the reasons to help and look at the incubation success rate and sex determination of sea turtles. Though the maps don't help to get the temperatures at depths which mimic the sea turtle incubation chambers but it does help with the surface temperature knowledge which is important to know as the surface temperature induces the heat to the depths. The in-situ field measurements do not provide with the surface temperatures and it is also important to note that collecting large data with field measurements takes a lot a human power and days to obtain the data. The study shows that the surface temperature of the study area (Figure 1) indicates hotter temperature at the developed and more populated areas shown in red, medium temperatures (yellow) at low populated and cooler temperatures (blue) at sea waters and lakes. The closer zoom into the Jupiter North beach location in Figure 2 shows that the temperatures are ranging from 80.33 °F to 89.33 °F which is coinciding with the field measurements obtained at 45 cm depth as 88.51 °F and 87.77 °F respectively for Mid beach and Dune toe. The slight variation is due to the difference in data collected day and also the comparison of surface temperature to the temperatures at 45 cm depth. The reflectance curves

support the low temperatures with the high reflectance for JN_H45 and vice-versa for JN_M45. The whole study shows that the remote sensing and its applications by using the satellite images help to obtain vast data and can be analyzed without getting out for the field data. Though the field data for at least for couple of locations is important to correlate the satellite data as done in this project, however, it decreases the amount of data to be collection.

REFERENCES

Angilletta MJ, Niewiarowski PH, Navas CA, 2002 The evolution of thermal physiology in ectotherms. Journal of Thermal Biology 27: 249–268.

Angilletta MJ, Steury TD, Sears MW, 2004 Temperature, growth rate, and body size in ectotherms: fitting pieces of a life-history puzzle. Integrative and Comparative Biology 44: 498–509.

B. Dousset, 1991. Surface temperature statistics over Los Angeles: the influence of land use. Proc. IGARSS, Helsinki, Finland, pp. 367-371.

Brown JH, Gillooly JF, Allen AP, Savage VM, West GB, 2004. Toward a metabolic theory of ecology. Ecology 85: 1771–1789.

Crago, R. D., & Qualls, R. J. 2014. Use of land surface temperature to estimate surface energy fluxes: Contributions of Wilfried Brutsaert and collaborators. *Water Resources Research*, **50**, 3396– 3408.

D.A. Quattrochi, M.K. Ridd, 1994. Measurement and analysis of thermal energy responses for discrete urban surfaces using remote sensing data. International Journal of Remote Sensing, 15 (10), pp. 1991-2022.

F. Becker and Z.-L. Li, 1990, Towards a local split window method over land surfaces, International Journal of Remote Sensing, vol. 11, no. 3, pp. 369–393.

http://www.shadedrelief.com/landsat8/introduction.html

Huey RB, Stevenson RD, 1979 Integrating thermal physiology and ecology of ectotherms: discussion of approaches. American Zoologist 19: 357–366.

J.A. Voogt, T.R. Oke, 1998. Effects of urban surface geometry on remotely-sensed surface temperature. International Journal of Remote Sensing, 19 (5) (1998), pp. 895-920.

Kalnay E, Cai M, 2003. Impact of urbanization and land-use on climate. Nature 423:528–531

L. A. Hawkes, A. C. Broderick, M. H. Godfrey, B. J. Godley, 2007. Investigating the potential impacts of climate change on a marine turtle population. Global change biology

M. Roth, T.R. Oke, W.J. Emery, 1989. Satellite derived urban heat islands from three coastal cities and the utilization of such data in urban climatology. International Journal of Remote Sensing, 10 (11), pp. 1699-1720.

Oke TR, 1973. City size and the urban heat island. Atmospheric Environment 7: 769–779.

Oke TR, 1987. Boundary layer climates, 2nd edn. Routledge, London

Quattrochi DA, Ridd MK, 1994. Measurements and analysis of thermal energy responses from discrete urban surfaces using remote sensing data. Int J Remote Sens 15:1991–2002

R.C. Balling, S.W. Brazel, 1988. High-resolution surface temperature patterns in a complex terrain Photogrammetric Engineering and Remote Sensing, 54 (9), pp. 1289-1293.

Roth M, 2002. Effects of cities on local climates. Arlington Institute for Global Environmental Strategies. pp. 1–13.

S. Ustin, 2004. Manual of Remote Sensing: Remote Sensing for Natural Resource Management and Environmental Monitoring, John Wiley & Sons, Hoboken, NJ, USA.

Savage V.M., Gillooly J.F., Brown J.H., West G.B., Charnov E.L, 2004 Effects of body size and temperature on population growth. American Naturalist 163: E429–E441

T.N. Carlson, J.K. Dodd, S.G. Benjamin, J.M. Cooper, 1981. Satellite estimation of surface energy balance, moisture availability and thermal inertia. Journal of Applied Meteorology, 20 (1), pp. 67-87.

T.W. Owen, T.N. Carlson, R.R. Gillies, 1998. **An assessment of satellite remotely-sensed land cover parameters in quantitatively describing the climatic effect of urbanization.** International Journal of Remote Sensing, 19 (9), pp. 1663-1681.

USGS Landsat 8 Level 1 info (https://www.usgs.gov/land-resources/nli/landsat/using-usgs-landsat-level-1-data-product).

USGS Landsat 8 resources (https://www.usgs.gov/land-resources/nli/landsat/landsat-8?qt-science_support_page_related_con=0#qt-science_support_page_related_con)

Wiens JJ, Graham CH, Moen DS, Smith SA, Reeder TW, 2006. Evolutionary and ecological causes of the latitudinal diversity gradient in hylid frogs: treefrog trees unearth the roots of high tropical diversity. American Naturalist 168: 579–596.4

APPENDIX 1

#	Date Time, GMT-04:00	Temp_M45	Temp_H45
2923	9/4/2016 0:13	88.579	87.71
2924	9/4/2016 0:28	88.626	87.71
2925	9/4/2016 0:43	88.626	87.71
2926	9/4/2016 0:58	88.626	87.71
2927	9/4/2016 1:13	88.626	87.757
2928	9/4/2016 1:28	88.626	87.757
2929	9/4/2016 1:43	88.626	87.802
2930	9/4/2016 1:58	88.626	87.802
2931	9/4/2016 2:13	88.626	87.802
2932	9/4/2016 2:28	88.626	87.802
2933	9/4/2016 2:43	88.626	87.802
2934	9/4/2016 2:58	88.626	87.802
2935	9/4/2016 3:13	88.626	87.802
2936	9/4/2016 3:28	88.626	87.802
2937	9/4/2016 3:43	88.626	87.802
2938	9/4/2016 3:58	88.626	87.847
2939	9/4/2016 4:13	88.579	87.847
2940	9/4/2016 4:28	88.579	87.847
2941	9/4/2016 4:43	88.579	87.847
2942	9/4/2016 4:58	88.579	87.847
2943	9/4/2016 5:13	88.534	87.847
2944	9/4/2016 5:28	88.534	87.802
2945	9/4/2016 5:43	88.534	87.802
2946	9/4/2016 5:58	88.488	87.802
2947	9/4/2016 6:13	88.488	87.802

2948	9/4/2016 6:28	88.488	87.802
2949	9/4/2016 6:43	88.443	87.802
2950	9/4/2016 6:58	88.443	87.802
2951	9/4/2016 7:13	88.396	87.802
2952	9/4/2016 7:28	88.396	87.802
2953	9/4/2016 7:43	88.396	87.802
2954	9/4/2016 7:58	88.351	87.757
2955	9/4/2016 8:13	88.351	87.757
2956	9/4/2016 8:28	88.306	87.757
2957	9/4/2016 8:43	88.306	87.757
2958	9/4/2016 8:58	88.259	87.71
2959	9/4/2016 9:13	88.259	87.71
2960	9/4/2016 9:28	88.214	87.71
2961	9/4/2016 9:43	88.214	87.71
2962	9/4/2016 9:58	88.167	87.665
2963	9/4/2016 10:13	88.167	87.665
2964	9/4/2016 10:28	88.122	87.665
2965	9/4/2016 10:43	88.122	87.62
2966	9/4/2016 10:58	88.075	87.62
2967	9/4/2016 11:13	88.075	87.62
2968	9/4/2016 11:28	88.03	87.62
2969	9/4/2016 11:43	88.03	87.573
2970	9/4/2016 11:58	87.985	87.573
2971	9/4/2016 12:13	87.985	87.528
2972	9/4/2016 12:28	87.939	87.528
2973	9/4/2016 12:43	87.939	87.528
2974	9/4/2016 12:58	87.894	87.528

2975	9/4/2016 13:13	87.894	87.483
2976	9/4/2016 13:28	87.894	87.483
2977	9/4/2016 13:43	87.894	87.483
2978	9/4/2016 13:58	87.894	87.483
2979	9/4/2016 14:13	87.894	87.436
2980	9/4/2016 14:28	87.894	87.436
2981	9/4/2016 14:43	87.894	87.436
2982	9/4/2016 14:58	87.894	87.436
2983	9/4/2016 15:13	87.894	87.436
2984	9/4/2016 15:28	87.939	87.436
2985	9/4/2016 15:43	87.939	87.436
2986	9/4/2016 15:58	87.985	87.436
2987	9/4/2016 16:13	88.03	87.483
2988	9/4/2016 16:28	88.03	87.483
2989	9/4/2016 16:43	88.075	87.483
2990	9/4/2016 16:58	88.122	87.528
2991	9/4/2016 17:13	88.167	87.528
2992	9/4/2016 17:28	88.214	87.528
2993	9/4/2016 17:43	88.259	87.573
2994	9/4/2016 17:58	88.351	87.62
2995	9/4/2016 18:13	88.396	87.62
2996	9/4/2016 18:28	88.443	87.665
2997	9/4/2016 18:43	88.534	87.71
2998	9/4/2016 18:58	88.579	87.71
2999	9/4/2016 19:13	88.671	87.757
3000	9/4/2016 19:28	88.718	87.802
3001	9/4/2016 19:43	88.81	87.847

3002	9/4/2016 19:58	88.855	87.894
3003	9/4/2016 20:13	88.947	87.939
3004	9/4/2016 20:28	89.04	87.985
3005	9/4/2016 20:43	89.085	88.03
3006	9/4/2016 20:58	89.177	88.075
3007	9/4/2016 21:13	89.269	88.075
3008	9/4/2016 21:28	89.316	88.167
3009	9/4/2016 21:43	89.362	88.214
3010	9/4/2016 21:58	89.454	88.259
3011	9/4/2016 22:13	89.499	88.306
3012	9/4/2016 22:28	89.546	88.351
3013	9/4/2016 22:43	89.638	88.396
3014	9/4/2016 22:58	89.685	88.396
3015	9/4/2016 23:13	89.731	88.443
3016	9/4/2016 23:28	89.776	88.488
3017	9/4/2016 23:43	89.823	88.534
3018	9/4/2016 23:58	89.87	88.579
	Average temp	88.506	87.772